

Enhanced seasonal forecast skill following stratospheric sudden warmings

Article

Accepted Version

Sigmond, M., Scinocca, J. F., Kharin, V. V. and Shepherd, T. G. ORCID: <https://orcid.org/0000-0002-6631-9968> (2013) Enhanced seasonal forecast skill following stratospheric sudden warmings. *Nature Geoscience*, 6 (2). pp. 98-102. ISSN 1752-0908 doi: <https://doi.org/10.1038/NGEO1698> Available at <https://centaur.reading.ac.uk/30624/>

It is advisable to refer to the publisher's version if you intend to cite from the work. See [Guidance on citing](#).

To link to this article DOI: <http://dx.doi.org/10.1038/NGEO1698>

Publisher: Nature Publishing

All outputs in CentAUR are protected by Intellectual Property Rights law, including copyright law. Copyright and IPR is retained by the creators or other copyright holders. Terms and conditions for use of this material are defined in the [End User Agreement](#).

www.reading.ac.uk/centaur

CentAUR

Central Archive at the University of Reading

1 **Enhanced seasonal forecast skill following stratospheric sudden warmings**

2

3 M. Sigmond^{1*}, J. F. Scinocca², V. V. Kharin², T. G. Shepherd^{1,3}

4

5

6

7

8 ¹Department of Physics, University of Toronto, Toronto, Ontario, Canada.

9 ²Canadian Centre for Climate Modelling and Analysis, Environment Canada, Victoria, British
10 Columbia, Canada

11 ³Department of Meteorology, University of Reading, Reading, United Kingdom.

12

13

14

15

16 * E-mail: sigmond@atmosphysics.utoronto.ca

17 *Submitted to Nature Geoscience, July 2012 – Revised October 2012*

18 Advances in the field of seasonal forecasting have brought widespread socio-economic benefits.
19 However, seasonal forecast skill in the extratropics is relatively modest¹, which has prompted the
20 seasonal forecasting community to search for additional sources of predictability^{2,3}. For over a
21 decade it has been suggested that the stratosphere can act as a source of enhanced seasonal
22 predictability, as long-lived circulation anomalies in the lower stratosphere following
23 Stratospheric Sudden Warmings are associated with same-signed circulation anomalies in the
24 troposphere for up to two months^{4,5}. Here we show that such enhanced predictability can be
25 realized in a dynamical seasonal forecast system, thus opening the door to prediction of a
26 comprehensive suite of parameters of socio-economic relevance. We employ a dynamical
27 forecast system with a good representation of the stratosphere to perform ensemble model
28 forecasts initialized at the onset date of Stratospheric Sudden Warmings. Our model forecasts
29 faithfully reproduce the observed mean tropospheric response in the following months, with
30 enhanced forecast skill of atmospheric circulation patterns, surface temperature over Northern
31 Russia and Eastern Canada, and North Atlantic precipitation. Our results imply that seasonal
32 forecast systems are likely to produce significantly higher forecast skill for certain regions when
33 initialized during Stratospheric Sudden Warmings.

34

35

36 Skillful seasonal forecasts rely on the predictability of slowly-varying components of the climate
37 system, such as sea surface temperature (SST), sea ice, snow, and soil moisture. Most of the skill
38 that is currently obtained by seasonal forecast systems stems from the predictability of El Niño
39 Southern Oscillation (ENSO) and its remote influences¹. In general, ENSO's influence declines

40 with increasing distance from the tropical Pacific Ocean, resulting in relatively smaller forecast
41 skill for the extratropics, especially over Northern Eurasia^{1,2}. However, two recent reports^{2,3} have
42 suggested that the maximum seasonal forecast skill has not been achieved, and have identified
43 the stratosphere as an untapped source of enhanced seasonal predictability. This is based on the
44 observation that rapid breakdowns of the westerly flow (or polar vortex) in the polar winter
45 stratosphere (known as Stratospheric Sudden Warmings or SSWs) tend to be followed by a
46 tropospheric circulation pattern that is often described as the negative phase of the Northern
47 Annular Mode (NAM)⁴, with a corresponding signature in surface temperature that is
48 complementary to that of ENSO (i.e. strongest over the Atlantic sector and Northern Eurasia,
49 where the ENSO impact is modest)⁵. However, SSWs are highly nonlinear events that are only
50 predictable a week or two in advance^{6,7}. Consequently, the enhanced seasonal predictability
51 coming from the stratosphere is likely to be conditional (i.e., only after a SSW has occurred).

52

53 Previous studies of enhanced seasonal predictability associated with SSWs are mainly based on
54 simple statistical models⁸⁻¹¹. Seasonal forecast systems based on dynamical models are able to
55 capture the average tropospheric state following SSWs to some extent¹², but it is not evident that
56 this is associated with a detectable increase in forecast skill of surface weather¹³. Here we
57 demonstrate that a dynamical forecast system initialized at the time of a SSW is able to predict
58 the mean tropospheric circulation response in the following months. We also show that the
59 forecast skill of socio-economically relevant variables such as surface temperature and
60 precipitation is significantly enhanced relative to the forecast skill in a set of unconditional
61 forecasts (i.e. control forecasts that are not explicitly initialized during SSWs).

62

63 The dynamical forecast system in this study employs the Canadian Middle Atmosphere Model
64 (CMAM)¹⁴. Retrospective forecasts (also known as hindcasts) are initialized at 20 SSW dates
65 between 1970 and 2009 (hereafter referred to as the SSW forecasts), each consisting of 10
66 ensemble members. In all model forecasts, SST anomalies that occur at initialization time are
67 thereafter relaxed to climatology as described in the Methods section. This allows us to exclude
68 predictability that may arise from SSTs (e.g., related to the ENSO phenomenon), thus isolating
69 predictability that stems from atmospheric and associated land initializations. We focus on the
70 ensemble mean forecast averaged over the 16-60 days after the SSWs. Forecast anomalies are
71 defined as differences relative to the climatology of the unforced (freely running) model (see the
72 Methods section).

73

74 The model prediction of the anomalous tropospheric state following SSWs agrees very well with
75 observations (Fig. 1; see also Supplementary Fig. S1). Figs. 1a and 1c (contours) show that
76 averaged over all 20 SSW cases, the observed Sea Level Pressure (SLP) pattern is characterized
77 by a dipole with anomalously high SLP at high latitudes and anomalously low SLP at mid-
78 latitudes. This pattern is often described as a negative NAM pattern. It is well reproduced by the
79 model (Figs. 1b and 1d), except that the centre of anomalously low SLP in the North Atlantic is
80 shifted east relative to that in the observations. The negative NAM pattern is associated with a
81 near-surface easterly wind anomaly at NH mid-latitudes (not shown), which results in increased
82 (decreased) advection of relatively warm ocean air to Eastern Canada (Northern Russia)¹⁵. The
83 resulting warm anomaly over Eastern Canada and cold anomaly over Northern Russia (Fig. 1a)

84 is again well captured by the model (Fig. 1b). The negative NAM pattern is also consistent with
85 an equatorward shift of the storm track (not shown), which is associated with decreased
86 precipitation (PCP) over the high-latitude Atlantic, and increased PCP over the mid-latitude
87 Atlantic (Fig. 1c). This feature is again well reproduced by the model (Fig. 1d), except that,
88 consistent with the SLP, the centre of anomalously high PCP in the mid-latitude North Atlantic is
89 shifted east relative to that in the observations.

90

91 The implications for forecast skill can be understood by considering Fig. 2a. It shows a scatter
92 plot of the observed versus forecast NAM index at 1000 hPa, where each point represents one
93 (ensemble mean) model forecast initialized at a particular SSW date. Most points are located in
94 the lower left quadrant, reflecting the fact that on average both the observed and modeled surface
95 NAM following the SSWs is negative. The average horizontal location (represented by the
96 vertical dashed line) is the mean observed value (-0.44). The horizontal error bar shows that the
97 observed mean surface NAM response is statistically significant at the 95% confidence level.
98 The average modeled surface NAM, which is the average vertical location of the points, is
99 somewhat larger (-0.74) and also statistically significant. The correlation between observed and
100 modeled surface NAM (hereafter referred to as the Correlation Skill Score (CSS) or simply
101 ‘forecast skill’) is substantial ($r=0.55$) and statistically significant at the 99% confidence level
102 (see also Fig. 4a), which is a reflection of the tendency of the points in the scatter plot to be
103 shifted towards the lower left quadrant. Thus, we find that our model has a significant skill in
104 forecasting the surface circulation for a lead time of 16-60 days.

105

106 Some of the skill in the SSW forecasts may, in principle, also stem from predictability of slowly
107 varying boundary conditions such as soil moisture (as noted above, the model forecasts are
108 designed to exclude SST effects on predictability). To quantify such skill, we performed a
109 control set of forecasts initialized at the same calendar dates as the SSWs, but in the year
110 preceding and the year following the SSWs. The results are plotted in Fig. 2b. We find a similar
111 spread in the observed and modeled surface NAM index as in the SSW forecasts, but instead of
112 being shifted towards a particular quadrant, the cloud of points is centered near the origin. The
113 near-zero (-0.01) CSS for the surface NAM demonstrates that the unconditional control forecasts
114 do not contain any forecast skill for the surface circulation for a lead time of 16-60 days,
115 demonstrating that the skill in the SSW forecasts does come from the SSWs themselves. Note
116 that the similar spread in the cloud of points in Figures 2a and 2b suggests that the inherent
117 predictability of the surface NAM is not enhanced after SSWs, but instead that the increased
118 correlation skill score in the SSW forecasts is largely due to the shift in the mean NAM towards
119 negative values.

120

121 The vertical profile of the mean NAM index following the SSWs is well captured by the model
122 forecasts (Fig. 3a). The model slightly overestimates the mean NAM response near the surface,
123 but correctly captures the vertical structure which maximizes in the lower stratosphere and
124 exhibits a minimum in the middle troposphere. The corresponding forecast skill is shown in Fig.
125 3b. Consistent with Fig. 2, it shows that near the surface the forecast skill is substantial and
126 significant for the SSW forecasts, and near-zero and not significant for the control forecasts.
127 Except for the mid to upper troposphere, forecast skill of the NAM following SSWs is

128 substantial, statistically significant, and significantly larger than in forecasts that are not
129 constrained to be initialized during SSWs.

130

131 The influence of SSWs on forecast skill for the NAM index and for Northern Hemisphere
132 surface variables is summarized in Fig. 4. The statistical significance of the difference between
133 the CSS in the SSW and control forecasts is labeled by p-values in this figure, which represent
134 the confidence level at which enhanced forecast skill can be associated with SSWs and which are
135 determined by bootstrapping. This level exceeds 99% ($p<0.01$) for the NAM at 100 and 1000
136 hPa (Fig. 4a), and is 98% for the North Atlantic Oscillation (NAO) (which is the local Atlantic
137 manifestation of the surface NAM and is defined here as the SLP difference between Iceland and
138 the Azores) (Fig. 4b). For SLP, Surface Temperature (ST) and PCP, forecast skill averaged over
139 20-90°N (left bars in Figs. 4b-d) is statistically significant in the SSW forecasts, and enhanced
140 relative to that in the control forecasts. However, this enhancement is only statistically
141 significant for SLP ($p=0.04$). Focusing on localized regions, significant skill enhancement can be
142 detected for ST in Northern Russia and Eastern Canada (Fig. 4c) and for the PCP gradient over
143 the Northern Atlantic (Fig. 4d).

144

145 For more than a decade it has been suggested that the stratosphere can act as a source of seasonal
146 predictability. The results in this paper confirm that such predictability can be realized in
147 dynamical forecast systems. A requirement for the predictability to be realized is a model that
148 realistically simulates the tropospheric response to SSWs. Even though current seasonal forecast

149 systems (which generally have a poorly represented stratosphere) capture this response with
150 some credibility¹², it has been suggested that the response is more realistic in models with a well-
151 represented stratosphere¹⁶ such as the model employed here. Also, as SSWs themselves are
152 better predicted with a longer lead time in such models⁷ it may be possible to elevate seasonal
153 forecast skill by raising the model lid and increasing vertical resolution in the stratosphere^{2,17}.

154

155 In assessing the practical implications of these results it must be noted that the enhanced
156 predictability is highly conditional and contingent upon the occurrence of SSWs, which occur on
157 average in six out of ten winters. Although the seasonal predictability associated with ENSO is
158 also conditional, there are two important differences: 1) SSWs are inherently less predictable
159 than ENSO giving a shorter lead time for the opportunity, and 2) the window of opportunity is
160 comparatively limited as the SSW influence on the troposphere only lasts for about half to two-
161 thirds of a season. Therefore the potential enhancement of forecast skill associated with SSWs is
162 likely to be very limited in standard seasonal forecasts which are generally issued once a month.

163 In an attempt to exploit this source of predictability stemming from the stratosphere, seasonal
164 forecast centers could issue special forecasts once a SSW has been identified in observations.
165 This would require additional computational resources as forecast simulations initialized at non-
166 standard dates would have to be performed. The results presented here suggest that such
167 additional computational effort would be well justified, as the special forecasts are likely to
168 feature enhanced forecast skill with potentially widespread socio-economic benefits.

169

170 **Methods**

171 **Observational dataset and model forecasts**

172 The 1970-1988 data from ERA-40 (ref. 18) and the 1989-2009 data from ERA-Interim¹⁹ are
173 merged to provide an observational dataset that is used to initialize and verify the model. To
174 identify Stratospheric Sudden Warmings (SSWs), we apply a criterion based on the Northern
175 Annular Mode (NAM) index instead of the standard WMO criterion which is based on the zonal-
176 mean zonal wind at 10 hPa and 60°N, as the NAM index has been shown to better gauge
177 stratosphere-troposphere coupling than zonal-mean zonal wind²⁰. A SSW is defined to occur
178 when the NAM index calculated from year-round daily zonal-mean geopotential height
179 following ref. 20 first drops below -2.5 at 30 hPa. For winters with multiple SSWs, we only
180 consider the warming with the largest amplitude. Following this procedure 20 warming cases are
181 found between November 1970 and March 2009.

182

183 The dynamical seasonal forecast system is based on the Canadian Middle Atmosphere Model
184 (CMAM)¹⁴, which has 71 vertical levels from the surface up to about 100 km at T63 horizontal
185 resolution. To assess the forecast skill following SSWs we performed 10-member ensemble
186 model forecasts initialized at the 20 SSW dates identified from the observations. The 10 initial
187 states for each SSW are obtained as follows. Ten model runs are started from 10 slightly
188 different atmospheric states on January 1, 1970. In these ‘assimilation’ runs, the spatial scales of
189 the vorticity, divergence and temperature that can be represented by spectral truncation T21 are
190 relaxed towards the time-evolving reanalyses between 1970 and 2009. The relaxation time is 24
191 hours, which is selected such that the simulated state closely follows the observed one, and the

192 resulting RMS spread between ensemble members roughly matches the RMS spread between the
193 different reanalysis data sets. The initial atmospheric and land conditions used for the model
194 forecasts at the onset date of the observed SSWs are obtained from these 10 assimilation runs.
195 The initial sea surface temperature (SST) and sea-ice fields are taken from the HadISST
196 dataset²¹. Instead of persisting the SST anomaly that occurs at initialization time for the duration
197 of the model forecast, which is common for operational two-tier seasonal forecasts, we linearly
198 relax the SST anomaly towards climatology in the first 2 weeks of the forecasts. We apply this
199 procedure to exclude predictability that may arise from SSTs, thus isolating the predictability
200 that stems directly from atmospheric perturbations (i.e., SSWs) alone.

201

202 To assess if the skill for the forecasts initialized during SSWs is significantly larger than a
203 typical, unconditional forecast, we performed a control set of forecasts initialized at the same
204 calendar dates as the SSWs, but in the year preceding and the year following the SSWs. For the
205 warming that occurred in the 1970-1971 (2008-2009) winter, the control forecast in only the
206 following (previous) winter is performed, as no initial conditions were available for the 1969-
207 1970 (2009-2010) winters. This results in 38 control forecasts, which are compared to the 20
208 SSW forecasts.

209

210 In order to calculate anomalies of meteorological fields in the forecast runs, a reference model
211 climatology must be defined. For this purpose, we performed 10-member ensemble model
212 simulations for the period 1970-2009 with prescribed HadISST SST and sea-ice fields, referred
213 to as AMIP runs. Anomalies of sea level pressure (SLP), Surface Temperature (ST) and
214 Precipitation (PCP) in the model forecasts are calculated relative to the corresponding ensemble

215 mean climatologies in these AMIP runs. The daily NAM index in the model forecasts is obtained
216 by projecting zonal mean geopotential height anomalies relative to the corresponding AMIP
217 climatology onto the observed NAM pattern. We note that during the first ~15 days of the
218 forecasts the model drifts from observations to the mean behaviour of the AMIP runs (see
219 Supplementary Material). Therefore our analysis focusses on days 16-60 after the SSWs.

220

221 **Forecast skill quantification**

222 The forecast skill is quantified by the Correlation Skill Score (CSS) defined as follows. Let F_m
223 represent the ensemble mean forecast of a variable (e.g., ST) averaged over a certain period (in
224 this paper, days 16-60) after the forecast initialization date indexed by $m = 1, \dots, M$, and X_m
225 represent the corresponding observed value. $M = 20(38)$ for the SSW (control) forecasts.

226 The CSS is given by:

227
$$CSS = \frac{Cov_{X,F}}{\sqrt{Var_X Var_F}},$$

228 where

229
$$Cov_{X,F} = \frac{1}{M} \sum_{m=1}^M X'_m F'_m ,$$

230
$$Var_X = \frac{1}{M} \sum_{m=1}^M X'^2_m ,$$

231
$$Var_F = \frac{1}{M} \sum_{m=1}^M F'^2_m .$$

232 For SLP, ST, and PCP, X'_m is the observed anomaly relative to the 1970-2009 observed
233 climatology, and F'_m is the model forecast anomaly relative to the climatology in the AMIP runs.
234 For the NAM index, X'_m and F'_m represent the values of the observed and forecast NAM index
235 itself since it is already calculated from anomalies of geopotential height. Statistical significance

236 of the CSS is determined in a bootstrapping procedure by random sampling with replacement of
237 M pairs of F'_m and X'_m .

238

239 **References**

- 240 1. Oldenborgh, G.J. van, Balmaseda, M., Ferranti, L., Stockdale, T.N. & Anderson, D.L.T.
241 Evaluation of atmospheric fields from the ECMWF seasonal forecasts over a 15-year
242 period. *J. Clim.* **18**, 3250-3269 (2005).
- 243 2. Kirtman, B. & Pirani, A. WCRP position paper on seasonal prediction. *WCRP Informal*
244 *Report 3*, (2008).
- 245 3. NRC, *Assessment of Intraseasonal to Interannual Climate Prediction and Predictability*
246 (National Academies Press, 2010).
- 247 4. Baldwin, M.P. & Dunkerton, T.J. Stratospheric harbingers of anomalous weather
248 regimes. *Science* **294**, 581-4 (2001).
- 249 5. Thompson, D.W.J., Baldwin, M.P. & Wallace, J.M. Stratospheric Connection to
250 Northern Hemisphere Wintertime Weather: Implications for Prediction. *J. Clim.* **15**,
251 1421-1428 (2002).
- 252 6. Gerber, E.P., Orbe, C. & Polvani, L.M. Stratospheric influence on the tropospheric
253 circulation revealed by idealized ensemble forecasts. *Geophys. Res. Lett.* **36**, L24801
254 (2009).

- 255 7. Marshall, A.G. & Scaife, A.A. Improved predictability of stratospheric sudden warming
256 events in an atmospheric general circulation model with enhanced stratospheric
257 resolution. *J. Geophys. Res.* **115**, D16114 (2010).
- 258 8. Baldwin, M.P. *et al.* Stratospheric memory and skill of extended-range weather forecasts.
259 *Science* **301**, 636-40 (2003).
- 260 9. Charlton, A.J., O'Neill, A., Stephenson, D.B., Lahoz, W.A. & Baldwin, M.P. Can
261 knowledge of the state of the stratosphere be used to improve statistical forecasts of the
262 troposphere? *Q. J. R. Meteorol. Soc.* **129**, 3205-3224 (2003).
- 263 10. Christiansen, B. Downward propagation and statistical forecast of the near-surface
264 weather. *J. Geophys. Res.* **110**, D14104 (2005).
- 265 11. Siegmund, P. Stratospheric polar cap mean height and temperature as extended-range
266 weather predictors. *Mon. Weather Rev.* **133**, 2436-2448 (2005).
- 267 12. Maycock, A.C., Keeley, S.P.E., Charlton-Perez, A.J. & Doblas-Reyes, F.J. Stratospheric
268 circulation in seasonal forecasting models: implications for seasonal prediction. *Clim.*
269 *Dyn.* **36**, 309-321 (2011).
- 270 13. Mukougawa, H., Hirooka, T. & Kuroda, Y. Influence of stratospheric circulation on the
271 predictability of the tropospheric Northern Annular Mode. *Geophys. Res. Lett.* **36**,
272 L08814 (2009).
- 273 14. Scinocca, J.F., McFarlane, N. A., Lazare, M., Li, J. & Plummer, D. Technical Note: The
274 CCCma third generation AGCM and its extension into the middle atmosphere. *Atmos.*
275 *Chem. Phys.* **8**, 7055-7074 (2008).

- 276 15. Thompson, D.W. & Wallace, J.M. Regional climate impacts of the Northern Hemisphere
277 annular mode. *Science* **293**, 85-9 (2001).
- 278 16. Hardiman, S.C., Butchart, N., Hinton, T.J., Osprey, S.M. & Gray, L.J. The effect of a
279 well resolved stratosphere on surface climate: Differences between CMIP5 simulations
280 with high and low top versions of the Met Office climate model. *J. Clim.*, **25**, 7083–7099
281 (2012).
- 282 17. Roff, G., Thompson, D.W.J. & Hendon, H. Does increasing model stratospheric
283 resolution improve extended-range forecast skill? *Geophys. Res. Lett.* **38**, L05809 (2011).
- 284 18. Uppala, S.M. *et al.* The ERA-40 re-analysis. *Q. J. R. Meteorol. Soc.* **131**, 2961-3012
285 (2005).
- 286 19. Dee, D.P. *et al.* The ERA-Interim reanalysis: configuration and performance of the data
287 assimilation system. *Q. J. R. Meteorol. Soc.* **137**, 553-597 (2011).
- 288 20. Baldwin, M.P. & Thompson, D.W.J. A critical comparison of stratosphere–troposphere
289 coupling indices. *Q. J. R. Meteorol. Soc.* **135**, 1661–1672 (2009).
- 290 21. Rayner, N. A. *et al.* Global analyses of sea surface temperature, sea ice, and night marine
291 air temperature since the late nineteenth century. *J. Geophys. Res.* **108**, (D14), 4407
292 (2003).
- 293
- 294
- 295

296 **Figure 1 | Surface climate response to SSWs. a-d,** Mean anomaly averaged over days 16-60
297 after all SSWs of sea level pressure (contours), surface temperature (shading in **a** and **b**) and
298 precipitation (shading in **c** and **d**) for the observations (**a** and **c**) and the model forecasts (**b** and
299 **d**). Contour interval for sea level pressure is 1 hPa (...,-1.5,-0.5,0.5,...), and solid (dashed)
300 contours denote positive (negative) values. Black dots represent statistical significance at the
301 90% confidence level (determined by bootstrapping) of the shaded quantities. Observed
302 (modeled) SLP anomalies are generally significant at the 90% level where the mean anomaly
303 exceeds ~1.5 (0.5) hPa.

304

305 **Figure 2 | Observed versus forecast 1000 hPa NAM index. a-b,** Scatter plot of the observed
306 versus forecast NAM index at 1000 hPa averaged over 16-60 days following the 20 SSWs (**a**)
307 and the 38 control dates (**b**). The vertical dashed line and corresponding black dot represent the
308 average observed value, and the horizontal error bar and corresponding gray shading its 95%
309 confidence interval (as determined by bootstrapping). The horizontal dashed line and
310 corresponding black dot represent the average forecast value, and the vertical error bar and
311 corresponding gray shading its 95% confidence interval.

312

313

314

315 **Figure 3 | Vertical profile of the mean NAM and of the CSS of the NAM. a-b** The mean
316 NAM index averaged over 16-60 days after all SSWs (red) and the control dates (blue) as a
317 function of height for the observations (thick line) and the model forecasts (thin line) **(a)**. The
318 error bars represent the 95% confidence interval for the model forecast. The forecast skill as
319 quantified by the CSS as a function of height **(b)**. The difference between the SSW and control
320 CSS is statistically significant at the 95% level where the error bars do not overlap.

321

322 **Figure 4 | The CSS of various variables. a-d,** The CSS of the NAM at 100 and 1000 hPa **(a)**,
323 NAO index **(b)**, surface temperature (ST) over Northern Russia and Eastern Canada (indicated
324 by the blue boxes in Figs. 1a and 1b) **(c)**, precipitation (PCP) difference between the high latitude
325 and mid-latitude Northern Atlantic (indicated by the blue boxes in Figs. 1c and 1d) **(d)**, and the
326 CSS averaged over 20-90°N for SLP **(b)**, ST (land only) **(c)** and PCP **(d)**. Red (blue) bars
327 represent the SSW (control) forecasts for a forecast range of 16-60 days. The thin lines represent
328 the 95% confidence interval. P-values for the difference between the SSW and control CSS are
329 given. This difference is statistically significant at the 95% level when the thick brown lines do
330 not overlap.

331

332

333

334

335

336 **Correspondence**

337 Correspondence and requests for materials should be addressed to M.S. (email:
338 sigmond@atmosp.physics.utoronto.ca)

339 **Acknowledgments**

340 Michael Sigmond gratefully acknowledges funding by Environment Canada through a Grants
341 and Contributions Agreement with the University of Toronto. We thank Bill Merryfield, John
342 Fyfe and Nathan Gillett for their helpful comments.

343 **Author contributions**

344 M.S., J.F.S. and V.V.K. designed the experiments. All authors interpreted the results and
345 contributed to writing the paper.

346 **Additional Information**

347 Supplementary information accompanies this paper on www.nature.com/naturegeoscience.

348 **Competing financial interests**

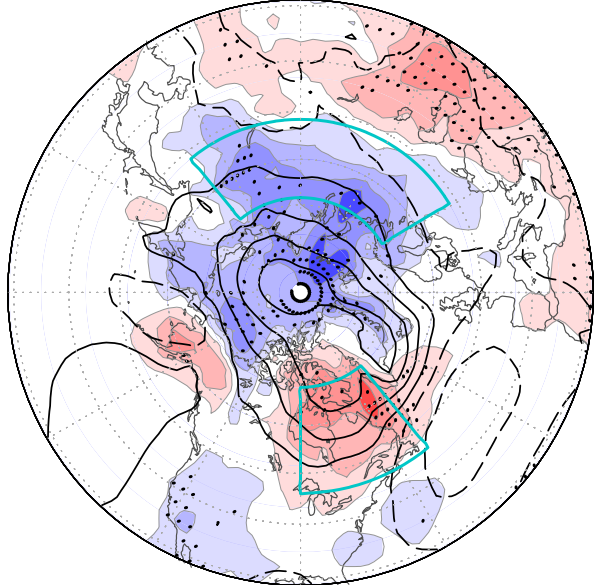
349 The authors declare no competing financial interests.

350

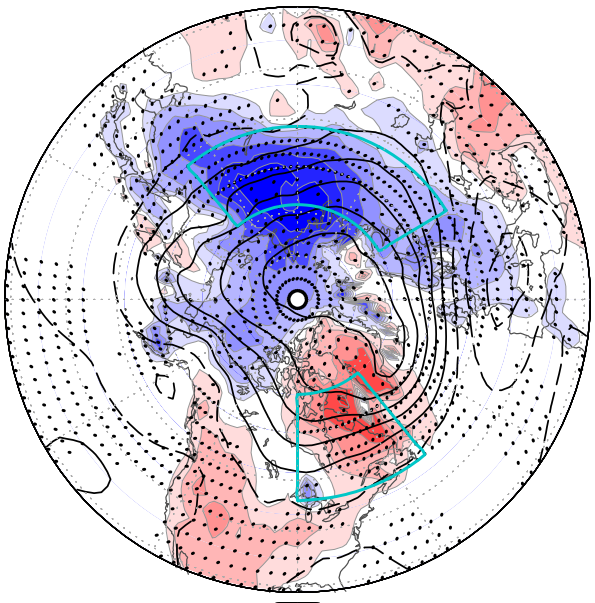
351

352

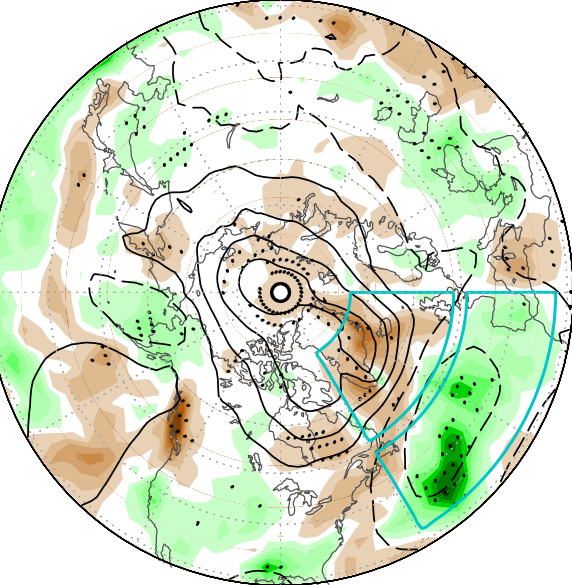
a SLP and ST (Observations)



b SLP and ST (Forecast)



c SLP and PCP (Observations)



d SLP and PCP (Forecast)

